Radial Basis Function (RBF) Network Adaptive Power System Stabilizer

Ravi Segal, M. L. Kothari, *Senior Member, IEEE*, and Shekhar Madnani

***Abstract*—This paper presents a new approach for real-time tuning the parameters of a conventional power system stabilizer (PSS) using a radial basis function (RBF) network. The RBF network is trained using an orthogonal least squares (OLS) learning algorithm. Investigations reveal that the required number of RBF centers depends on spread factor, β and the number of training patterns. Studies show that a parsimonious RBF network can be obtained by presenting a relatively smaller number of training patterns, generated randomly and spreadover the entire operating domain. Investigations reveal that the dynamic performance of the system with an RBF network adaptive PSS (RBFAPSS) is virtually identical to that of an artificial neural network based adaptive PSS (ANNAPSS). The dynamic performance of the system with RBFAPSS is quite robust over a wide range of loading conditions and equivalent reactance X_e.**

***Index Terms*—Power system stabilizer (PSS), Small signal stability, Radial basis function (RBF) network, Artificial neural network (ANN), Adaptive PSS.**

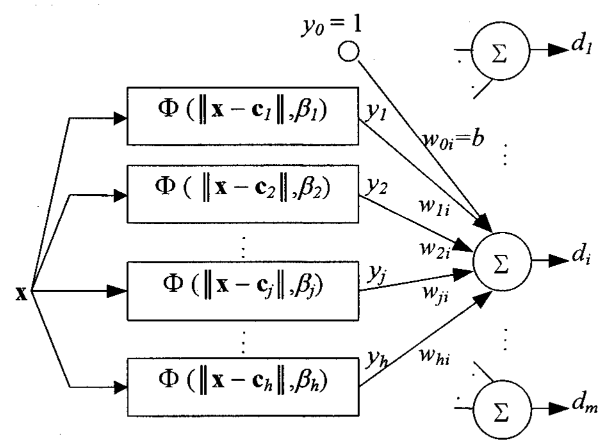

Fig. 1. A radial basis function neural network.

I. Introduction

POWER system stabilizers (PSS) have been extensively used in modern power systems for enhancing stability of the system. The conventional fixed structure PSS, designed using a linear model obtained by linearizing nonlinear model around a nominal operating point provides optimum performance for the nominal operating condition and system parameters. However, the performance becomes suboptimal following deviations in system parameters and loading condition from their nominal values.

In recent years self-tuning PSS, variable structure PSS, artificial neural network (ANN) based PSS and fuzzy logic PSS have been proposed to provide optimum damping to the system oscillations over a wide range of system parameters and loading conditions. Two reasons are put forward for using ANN. First, since an ANN is based on parallel processing, it can provide extremely fast processing facility. The second reason for the high level of interest is the ability of ANN to realize complicated nonlinear mapping from the input space to the output space.

In the ANN based PSS [4]–[7], the network is trained using back-propagation training algorithm. The training of feedforward ANN is based on nonlinear optimization technique and the parameter estimate may get trapped at a local minimum of the chosen optimization criterion during the learning procedure when the gradient descent algorithm is used. A viable alternative to highly nonlinear-in-the-parameter neural networks is the radial basis function (RBF) networks.

The performance of an RBF network critically depends upon the chosen RBF centers. Orthogonal Least Squares (OLS) algorithm [3] is very powerful in selecting required number of RBF centers. The use of OLS algorithm results in an adequate and parsimonious RBF network. No attempt seems to have been made to design an RBF network based adaptive PSS (RBFAPSS). Here, a maiden attempt has been made to design and study the performance of an RBFAPSS. The main objectives of the research work presented in this paper are:

1. To present a systematic approach for designing an RBFAPSS using an OLS training algorithm.
2. To study the dynamic performance of the system with RBFAPSS and hence to compare with that of ANN based adaptive PSS (ANNAPSS).
3. To investigate the effect of variation of loading condition and equivalent reactance, X_e on dynamic performance of the system with an RBFAPSS.

II. The Radial Basis Function Network

An RBF network has a feedforward structure consisting of a single hidden layer of h locally tuned units which are fully interconnected to an output layer of m linear units, as shown in Fig. 1. All hidden units simultaneously receive the p-dimensional real valued input vector $\boldsymbol{x}$. The input vector to the network is passed to the hidden layer nodes via unit connection weights. The hidden layer consists of a set of radial basis functions. Associated with ith hidden unit is a parameter vector, $\boldsymbol{c}_i$ called a

Manuscript received February 12, 1999; revised July 22, 1999. This work was supported by the Department of Science and Technology, Power Grid Corporation India Limited and ABB. The work of R. Segal was supported by the management of GE Power Services (I) Limited.

The authors are with the Department of Electrical Engineering, Indian Institute of Technology, Hauz Khas, New Delhi - 110 016, India.

Publisher Item Identifier S 0885-8950(00)04561-2.

center. The hidden layer node calculates the Euclidean distance between the center and the network input vector and then passes the result to the radial basis function. All the radial basis functions are, usually, of the same type. Thus the hidden layer performs a fixed nonlinear transformation and it maps the input space onto a new space. The output layer, then, implements a linear combiner on this new space and the only adjustable parameters are the weights of this linear combiner. These parameters can be determined using the linear least squares method, which is an important advantage of this method.

In this network, provision is made for a bias (i.e., data independent variable) applied to the output unit. This is done simply by setting one of the linear weights of each of the nodes in the output layer of the network equal to the bias and treating the associated radial basis function as a constant equal to 1.

An RBF network is designed to perform a nonlinear mapping from the input space to the hidden space, followed by a linear mapping from the hidden space to the output space. Thus, in an overall fashion, the network represents a map from the p-dimensional input space to m-dimensional output space, written as S: $R^p \rightarrow R^m$ according to:

$$d_i = w_{0i} + \sum_{j=1}^{h} w_{ji}\, \Phi(\|\boldsymbol{x} - \boldsymbol{c}_j\|, \beta_j) \tag{1}$$

where, $i = 1, \ldots, m$ and $j = 1, \ldots, h$.

d_i is the ith output.
$\boldsymbol{x} \in R^p$ is the input vector.
w_{0i} is the biasing term.
h is the number of hidden units.
w_{ji} is the weight between the jth hidden node and the ith output node.
$\boldsymbol{c}_j \in R^p$ is the center of the jth hidden node.
β_j is the real constant known as spread factor.
$\Phi(.)$ is the nonlinear function.

In this study, $\Phi(.)$ is chosen to be the Gaussian function, that is for the jth hidden unit;

$$\Phi(z_j, \beta_j) = \exp(-z_j^2/\beta_j^2) \quad \text{where, } z_j = \|\boldsymbol{x} - \boldsymbol{c}_j\| \tag{2}$$

The degree of accuracy can be controlled by three parameters: the number of radial basis functions or hidden units, centers of the hidden units and the width (i.e., spread factor, β).

III. System Investigated

A single machine-infinite bus (SMIB) system is considered for the present investigations. A machine connected to a large system through a transmission line may be reduced by using Thevenin's equivalent of the transmission network external to the machine. Because of the relative size of the system to which the machine is supplying power, the dynamics associated with machine will cause virtually no change in the voltage and frequency of the Thevenin's voltage E_B (infinite bus voltage). The Thevenin equivalent impedance shall henceforth be referred to as equivalent impedance (i.e., $R_e + jX_e$). The nominal parameters and the nominal operating condition of the system are given in the Appendix. IEEE type ST1A model of static excitation system has been considered. Conventional PSS comprising cascade connected lead-lag networks with generator angular speed deviation ($\Delta\omega$) as input signal has been considered.

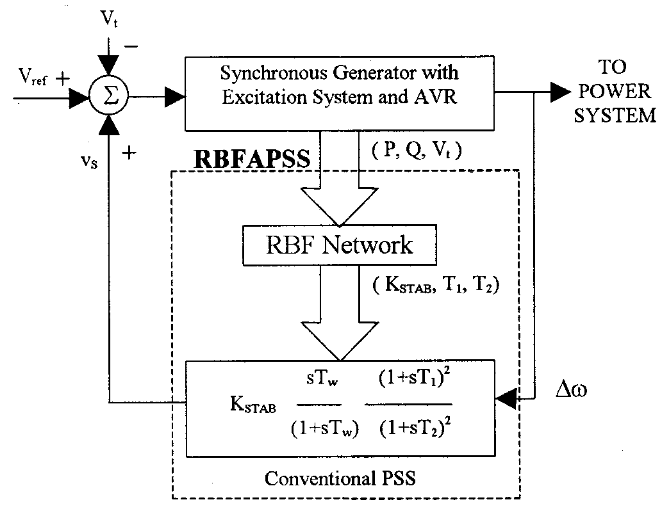

Fig. 2. Schematic diagram of a synchronous generator with RBFAPSS.

IV. RBF Network Adaptive PSS (RBFAPSS)

Fig. 2 shows the functional block diagram of the system with RBFAPSS. The output layer of the RBF network provides the desired PSS parameters (i.e., K_{STAB}, T_1 and T_2) in real-time. The input vector to the RBF network comprises generator real power output (P), reactive power output (Q) and terminal voltage (V_t).

V. Analysis

A. Generation of Training Patterns

The generator real power P, reactive power Q, and terminal voltage V_t are interrelated with infinite bus voltage E_B and equivalent reactance X_e. Considering $E_B = 1.0$ p.u., only three of the four parameters are independent. It may be noted that the desired domain of operation for a given system need be chosen carefully for generating training patterns. The P, V_t and X_e are assumed to vary over the ranges given below for the present investigations:

P: 0.5 to 1.0 p.u., V_t: 0.9 to 1.1 p.u., X_e: 0.4 to 0.8 p.u.

For each set comprising P, V_t and X_e, the value of Q is computed. The input vector of the training pattern is now P, Q and V_t. For each of these input vectors, the optimum parameters of the conventional PSS are computed using phase compensation technique [1], assuming a damping ratio $\zeta = 0.5$ for the electromechanical mode. The output vector of the training pattern, thus, becomes K_{STAB}^*, T_1^* and T_2^*. It is extremely important to highlight the significance of the choice of training pattern chosen. The training patterns account for the variation in equivalent reactance, X_e.

B. Design of RBF Network Adaptive PSS (RBFAPSS)

The input signals to an RBF network are the measurable quantities at the terminals of the synchronous generator

TABLE I
EFFECT OF VARIATION OF β ON REQUIRED NUMBER OF RBF CENTERS ($SSE = 0.1$)

β	0.03	0.04	0.05	0.06	0.075	0.08
No. of RBF Centers	247	213	186	165	164	171

(i.e., P, Q and V_t). This network computes, in real-time, the optimum parameters of the conventional PSS. The RBF network is trained using a function "SOLVERB" in NEURAL NETWORK TOOLBOX of the MATLAB software. The function "SOLVERB" implements orthogonal least squares (OLS) learning algorithm. The design of an RBF network for real-time tuning of the conventional PSS requires the selection of following parameters of the network:

1. The spread factor or width parameter β.
2. The number of RBF centers (nodes in the hidden layer) and their centers.
3. The bias vector and weighting matrix connecting hidden layer nodes to the output layer nodes.

For a given spread factor β, the orthogonal least squares (OLS) algorithm selects an optimum number of RBF centers from the training patterns presented to the network and estimates the bias vector and weighting matrix using least square error technique for the prescribed sum of squared errors (SSE). Following pertinent questions need be answered:

1. What is the effect of variation of β on the required number of RBF centers for a given value of SSE?
2. Is there any effect of variation of number of training patterns on the number of RBF centers chosen by OLS learning algorithm for a given value of SSE?

In order to answer the above questions, the following studies are carried out:

An RBF network is trained for $SSE = 0.1$ using OLS algorithm by presenting 400 training patterns (an arbitrarily chosen large number) for several values of β (Table I).

Examining Table I, it is clearly seen that β significantly affects the required number of RBF centers. For the typical problem investigated here, a minimum number of RBF centers equal to 164 is obtained for $\beta = 0.075$.

The effect of variation of number of training patterns on the minimum required number of RBF centers and corresponding β is examined by presenting several training sets with varying number of training patterns. For each training set, the value of β corresponding to minimum number of RBF centers is obtained (Table II). Further, in order to understand the effect of variation of number of RBF centers on robustness of the RBFAPSS, the critical clearing time (CCT) of the system with RBFAPSS is computed for the nominal operating condition and system parameters considering a 3-phase fault of transitory nature at the terminals of the generator (i.e., the post-fault system is same as the pre-fault one). The nonlinear mathematical model of the system as given in the Appendix is used for simulation studies. The variation of CCT with the variation of number of RBF centers is shown in Table II. The CCT attains a maximum value of 0.185 seconds for RBF centers equal to 4.

TABLE II
EFFECT OF VARIATION OF NUMBER OF TRAINING PATTERNS ON β, NUMBER OF RBF CENTERS TRAINING TIME AND CCT

No. of training patterns	Spread factor, β	No. of RBF Centers	Training Time (sec.)	CCT (sec.)
10	2.450	3	0.92	0.125
20	0.490	5	1.32	0.1525
40	0.395	4	1.32	0.185
60	0.275	7	2.19	0.175
80	0.450	8	2.70	0.175
100	0.875	15	5.30	0.175

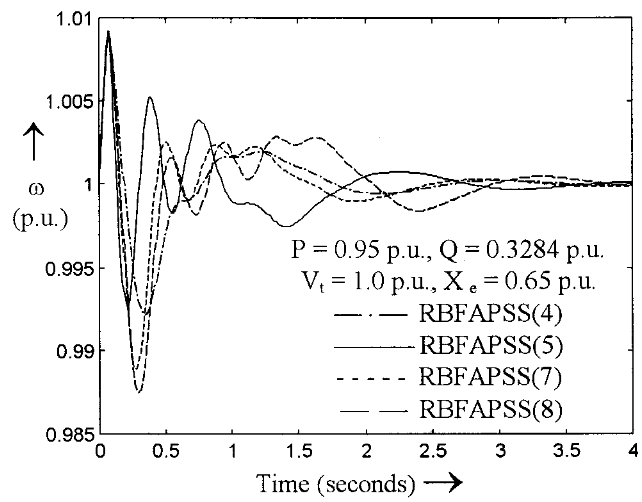

Fig. 3. Dynamic responses for ω considering different RBFAPSS.

How to select an adequate number of RBF centers? From the consideration of practical implementation, a smaller number of RBF centers is desirable. However, the primary consideration is the robustness of the resulting RBFAPSS. The RBF networks with reasonably small number of RBF centers i.e., 4, 5, 7 and 8 are chosen for further studies. For convenience of presentation, the RBFAPSS with 4, 5, 7 and 8 centers shall henceforth be denoted as RBFAPSS(4), RBFAPSS(5), RBFAPSS(7) and RBFAPSS(8) respectively.

C. Dynamic Performance of the System with RBFAPSS

Fig. 3 shows the dynamic responses for ω, with different RBFAPSS obtained for the nominal operating condition considering a transitory 3-phase fault of 4 cycles duration at the terminals of the generator.

Examining Fig. 3, it is clearly seen that the responses obtained with RBFAPSS(4) and RBFAPSS(5) hardly differ from each other in terms of peak deviations and settling time. However, the responses with RBFAPSS(7) and RBFAPSS(8) are slightly inferior to those obtained with RBFAPSS(4) and RBFAPSS(5). This clearly shows that an RBF network with larger number of RBF centers may not necessarily perform better.

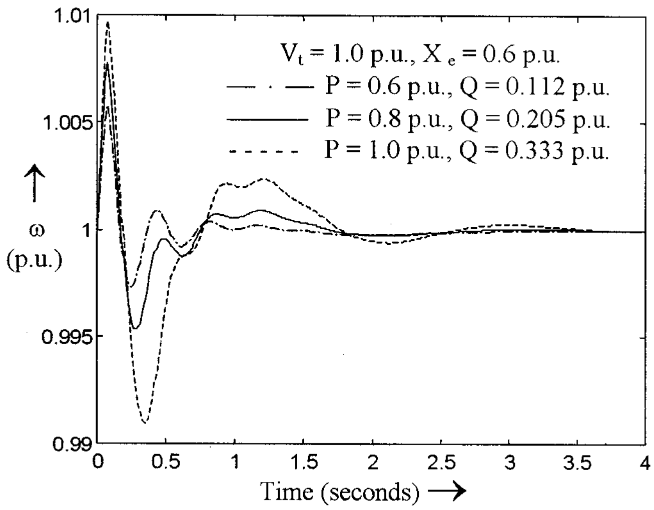

Fig. 4. Dynamic responses for ω for different loading conditions with RBFAPSS(5).

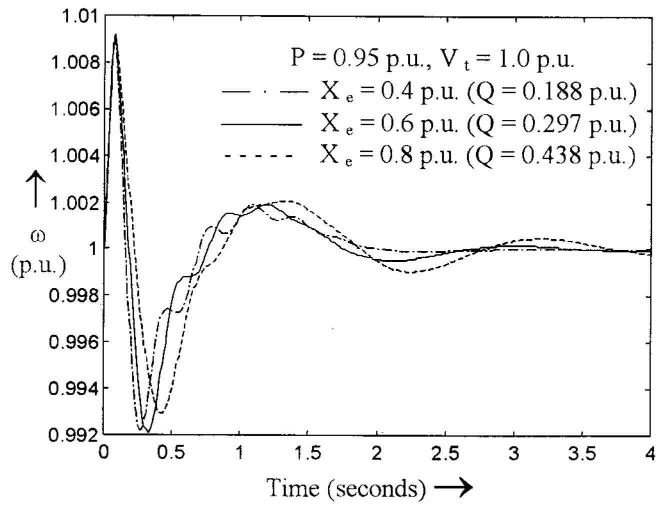

Fig. 5. Dynamic responses for ω for different values of X_e with RBFAPSS(5).

D. Effect of Variation of Loading Condition

The dynamic performance of the system with RBFAPSS is now evaluated considering a transitory 3-phase fault of 4 cycles duration at the terminals of the generator for the following five operating conditions uniformly spread over the input space:

1. $P = 0.6$ p.u., $Q = 0.112$ p.u. and $V_t = 1.0$ p.u.
2. $P = 0.8$ p.u., $Q = 0.205$ p.u. and $V_t = 1.0$ p.u.
3. $P = 1.0$ p.u., $Q = 0.333$ p.u. and $V_t = 1.0$ p.u.
4. $P = 1.0$ p.u., $Q = 0.232$ p.u. and $V_t = 0.9$ p.u.
5. $P = 1.0$ p.u., $Q = 0.480$ p.u. and $V_t = 1.1$ p.u.

$X_e = 0.6$ p.u. is chosen. Investigations reveal that the RBFAPSS(4), RBFAPSS(5) and RBFAPSS(7) exhibit quite a robust performance to wide variations in loading condition. However, the dynamic performance of the system with RBFAPSS(8) was relatively poor (dynamic responses not given here due to space constraint).

The performance of the RBFAPSS(4), RBFAPSS(5) and RBFAPSS(7) is further evaluated considering variation in X_e and a transitory 3-phase fault of 4 cycles duration at the terminals of the generator for the nominal operating condition. It was observed that the system becomes unstable when X_e is increased from 0.6 to 0.8 p.u. with RBFAPSS(4). The performances of RBFAPSS(5) and RBFAPSS(7) were found to be quite insensitive to wide variation in X_e from 0.4 to 0.8 p.u.

In view of the fact that the realization of an RBF network with 5 RBF centers is simpler and economical as compared to the one with 7 RBF centers, RBFAPSS(5) is chosen for further studies.

Fig. 4 shows the effect of variation of loading condition on dynamic performance of the system with RBFAPSS(5) considering a transitory 3-phase fault of 4 cycles duration.

It is quite clear (Fig. 4) that the dynamic performance of the system with RBFAPSS(5) is quite robust to wide variations in loading condition. The robustness of the RBFAPSS(5) is further examined considering wide variation in X_e. Fig. 5 clearly shows that RBFAPSS(5) is quite robust to variation in X_e over a wide range. Examining the responses (Figs. 4 and 5), it may be concluded that RBFAPSS(5) provides well damped responses for wide variations in the loading condition and equivalent reactance. Hence, RBFAPSS(5) may be recommended for practical implementation. The RBFAPSS(5) shall henceforth be denoted as RBFAPSS.

At this stage, a comprehensive comparison of the RBFAPSS with ANN based adaptive PSS (ANNAPSS) is desirable.

TABLE III
EFFECT OF VARIATION OF NUMBER OF NEURONS IN THE HIDDEN LAYER ON SSE, TRAINING TIME AND CCT

No. of neurons in the hidden layer	SSE	Training Time (sec.)	CCT (sec.)
4	0.357	191	0 .001
5	0.281	249	0.064
6	0.199	295	0.079
7	0.180	396	0.084
8	0.171	501	0.089
9	0.159	552	0.094
10	0.172	714	0.094

E. Design of ANN Based Adaptive PSS (ANNAPSS)

The architecture of the feedforward ANN comprises an input layer, one or more hidden layers and an output layer. For the present investigations, the elements of input vector are P, Q and V_t and that of the output vector are K^*_{STAB}, T^*_1 and T^*_2; and hence three neurons are needed in each of the input and the output layers. The ANN is trained presenting 400 training patterns using "TRAINLM" function of NEURAL NETWORK TOOLBOX of the MATLAB software. In order to arrive at an optimum number of neurons in the hidden layer, following systematic procedure is followed:

The effect of variation of number of neurons in the hidden layer on the performance of the ANNAPSS is evaluated. The following quantitative indices are considered for evaluating the performance of the ANNAPSS:

a) The value of SSE attained al the end of the ANN training.

TABLE IV
PARAMETERS OF THE CONVENTIONAL PSS COMPUTED USING RBF NETWORK, ANN AND CORRESPONDING OPTIMUM VALUES COMPUTED BY OFF-LINE STUDIES

Operating conditions (All values in p.u.)				PSS parameters computed using RBF network			PSS parameters computed using ANN			Optimum PSS parameters		
P	Q	V_t	X_e	K_{STAB}	T_1	T_2	K_{STAB}	T_1	T_2	K_{STAB}^*	T_1^*	T_2^*
0.73	0.07	0.94	0.56	21.09	0.333	0.065	21.56	0.334	0.064	21.52	0.334	0.064
0.97	0.27	0.99	0.55	21.05	0.336	0.068	22.58	0.330	0.064	22.59	0.329	0.064
0.76	0.19	0.95	0.76	21.81	0.347	0.085	22.31	0.348	0.086	22.15	0.347	0.086
0.99	0.23	0.93	0.58	18.73	0.360	0.079	17.53	0.358	0.076	17.98	0.359	0.076
0.85	0.15	0.96	0.56	20.01	0.338	0.068	21.56	0.335	0.065	21.45	0.335	0.065
0.87	0.07	0.91	0.52	18.71	0.346	0.063	17.98	0.351	0.064	18.22	0.353	0.064
0.60	0.22	1.06	0.56	36.59	0.307	0.069	35.81	0.304	0.063	35.74	0.300	0.057
0.86	0.28	0.98	0.71	22.38	0.343	0.083	22.88	0.340	0.081	22.78	0.341	0.081
0.86	0.28	1.02	0.65	24.39	0.330	0.074	25.46	0.325	0.071	25.35	0.326	0.071
0.90	0.19	0.90	0.65	17.28	0.368	0.089	17.34	0.366	0.086	17.35	0.371	0.087

b) The critical clearing time (CCT) of the system with ANNAPSS for a 3-phase transitory fault at the terminals of the generator for the nominal operating condition and parameters.

Table III shows the variation of SSE and CCT with the variation of number of neurons in the hidden layer. It is clearly seen that SSE decreases while CCT increases with the increase in number of neurons in the hidden layer. It is interesting to highlight the fact that with 9 neurons in the hidden layer, SSE attains a minimum value. The CCT becomes constant for number of neurons $\geq$9 in the hidden layer. Hence ANN with 9 neurons in the hidden layer is chosen for the ANNAPSS.

F. Comparison of RBFAPSS with ANNAPSS

Table IV shows the PSS parameters computed using RBF network and those computed using ANN for 10 typical operating conditions. The off-line computed optimum PSS parameters are also given in Table IV for the purpose of comparison. Examination of Table IV clearly shows that the PSS parameters computed with either RBF network or ANN are quite close to those computed by off-line studies.

Fig. 6 shows the dynamic responses for ω obtained with RBFAPSS and ANNAPSS considering a transitory 3-phase fault of 5 cycles duration at the terminals of the generator. It is clearly seen that the dynamic performance of RBFAPSS is virtually identical to that of ANNAPSS. It is important to highlight the fact that the robustness (no local minima problem) and quickness of learning are the most desirable features of a good learning algorithm. The OLS learning algorithm for the RBF network possesses both these features [3]. Tables II and III clearly show that the training of the RBF networks using OLS learning algorithm is much faster as compared to that of feedforward ANN using error back-propagation learning algorithm (computations were done using Pentium-100MHz PC). Further, examining Tables II and III, it may be seen that for the system investigated, CCT with RBFAPSS is quite large as compared to that with ANNAPSS. Thus, RBFAPSS is more robust as compared to ANNAPSS. It is extremely important to highlight the fact that the minimum value of SSE attained with ANN is 0.159 (implying local minimum) while RBF network can be trained for any value of SSE.

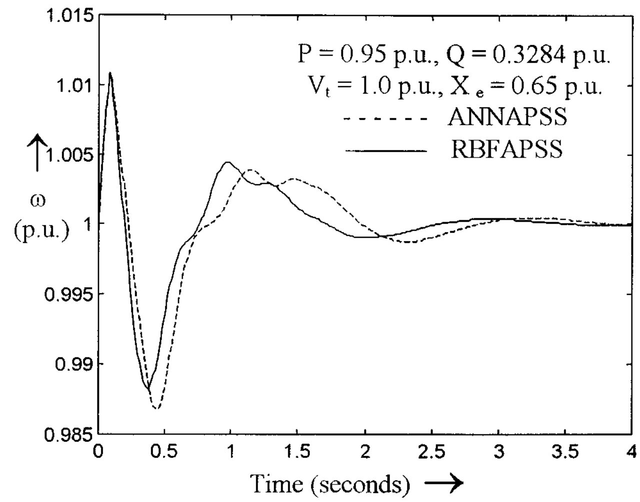

Fig. 6. Dynamic responses of the system for ω with ANNAPSS and RBFAPSS.

VI. CONCLUSIONS

The significant contributions of this paper are:

1. A new and simple approach for real-time tuning of conventional PSS using an RBF network has been proposed.
2. A systematic approach for designing an RBFAPSS using OLS algorithm has been presented.
3. Investigations reveal that the required number of RBF centers depends on spread factor β and number of training patterns. A parsimonious RBF network can easily be realized by presenting a relatively smaller number of training patterns.
4. Studies reveal that the dynamic performance of the system with RBFAPSS is virtually identical to that with ANNAPSS.
5. Investigations clearly show that the performance of an RBFAPSS is quite robust to wide variations in loading condition and X_e.

$M = 2H = 7.0,$	$P = 0.95,$	$V_t = 1.0,$	$E_B = 1.0,$
$X_d = 1.81,$	$X_q = 1.76,$	$X'_d = 0.3,$	$L_{adu} = 1.65,$
$X_1 = 0.16,$	$R_a = 0.003,$	$R_{fd} = 0.0006,$	$L_{fd} = 0.153,$
$K_A = 50,$	$T_R = 0.02,$	$T_A = 0.05,$	$X_e = 0.65,$
$R_e = 0.0,$	The system frequency $f_o = 60$ Hz.		

APPENDIX

The nominal parameters of the system are given at the top of the page. All data are in per unit, except M and the time constants. M and the time constants are expressed in seconds [2].

The nonlinear dynamic model of the system is given below.

$$\begin{aligned} \dot{\omega} &= (P_m - P_e)/2H \\ \dot{\delta} &= \omega_o(\omega - 1) \\ \dot{\Psi}_{fd} &= \omega_o R_{fd}(E_{fd}/L_{adu} - i_{fd}) \end{aligned}$$

For the nominal loading condition $E_{fd} = 2.506$ p.u. and $i_{fd} = 1.5161$ p.u.

NOMENCLATURE

H	Inertia constant
δ	Angle between quadrature axis and infinite bus voltage
ω	Angular speed
E_B	Infinite bus voltage
P_m, P_e	Mechanical and electrical powers respectively
L_{adu}	Unsaturated value of direct axis inductance
X_d	Direct axis reactance
X_q	Quadrature axis reactance
X'_d	Direct axis transient reactance
X_1	Leakage reactance
R_a	Stator resistance per phase
E_{fd}	Equivalent exciter voltage
Ψ_{fd}	Field winding flux linkages
T_R	Terminal voltage transducer time constant
V_{ref}	AVR reference signal
K_A, T_A	AVR gain and time constant respectively
v_S	Stabilizing signal
T_w	Washout time constant
K_{STAB}	PSS gain
$T_1 - T_2$	PSS time constants
i_{fd}	Field Current
R_{fd}, L_{fd}	Field winding resistance and inductance respectively
R_e, X_e	Equivalent resistance and reactance, respectively

REFERENCES

[1] Y.-N. Yu, *Electric power system dynamics*: Academic press, Inc., 1983.

[2] P. Kundur, *Power system stability and control*: McGraw Hill, Inc., 1994.

[3] S. Chen, C. F. N. Cowan, and P. M. Grant, “Orthogonal least squares learning algorithm for radial basis function networks,” *IEEE Transactions on Neural Networks*, vol. 2, no. 2, pp. 302–309, March 1991.

[4] Y.-Y Hsu and C.-R. Chen, “Tuning of power system stabilizers using an artificial neural network,” *IEEE Transactions on Energy Conversion*, vol. 6, no. 4, pp. 612–619, December 1991.

[5] Y. Zhang, G. P. Chen, O. P. Malik, and G. S. Hope, “An artificial neural network based adaptive power system stabilizer,” *IEEE Transactions on Energy Conversion*, vol. 8, no. 1, pp. 71–77, March 1993.

[6] L. Guan, S. Cheng, and R. Zhou, “Artificial neural network power system stabilizer trained with an improved BP algorithm,” *IEE Proceedings on Generation Transmission Distribution*, vol. 143, no. 2, pp. 135–141, March 1996.

[7] Y. M. Park and K. Y. Lee, “A neural network based power system stabilizer using power flow characteristics,” *IEEE Transactions on Energy Conversion*, vol. 11, no. 2, pp. 435–441, June 1996.

Ravi Segal received the B.E. degree in Electrical Engineering in 1983 and M.E. degree in Power Systems in 1988 from Punjab Engineering College, Chandigarh. He is a power plant professional and has been working in the area of generator protection, power plant controls, instrumentation and excitation systems.

He is working as Manager with GE Power Services (I) Limited and is closely associated with the practical implementation of various control schemes for thermal and hydro generators, particularly excitation systems. He is pursuing his Ph.D. research work at I.I.T. Delhi.

M. L. Kothari (SM’92), received the B.E. degree in Electrical Engineering from University of Jodhpur in 1964, M.E. degree in Power Systems from University of Rajasthan in 1970 and Ph.D. degree in 1981 from Indian Institute of Technology, New Delhi. He is a Professor at I.I.T. Delhi.

His research interests include Automatic Generation Control, Power System Stabilizers, Dynamic Security Analysis, Computer Relaying and application of Artificial Neural Network and Fuzzy logic control to power systems.

Shekhar Madnani received the B.E. degree in Electrical Engineering in 1996 from G. B. Pant University of Agriculture and Technology, Pantnagar.

He is a project scientist at I.I.T. Delhi and is working on a research project entitled “Tuning of power system stabilizers.”